Spectroscopic Signatures of Photocharging due to Hot-Carrier Transfer in Solutions of Semiconductor Nanocrystals under Low-Intensity Ultraviolet Excitation

John A. McGuire,[†,‡] Milan Sykora,[†] István Robel, Lazaro A. Padilha, Jin Joo,[§] Jeffrey M. Pietryga, and Victor I. Klimov*

Center for Advanced Solar Photophysics, Chemistry Division, Los Alamos National Laboratory, Los Alamos, New Mexico 87545, United States. [†]These authors contributed equally to this work. [‡]Present address: Department of Physics and Astronomy, Michigan State University, East Lansing, Michigan 48824, United States. [§]Present address: Department of Applied Chemistry, Kyungpook National University, Daegu, 702-701, South Korea.

ABSTRACT We show that excitation of solutions of well-passivated PbSe semiconductor nanocrystals (NCs) with ultraviolet (3.1 eV) photons can produce long-lived charge-separated states in which the NC core is left with a nonzero net charge. Since this process is not observed for lower-energy (1.5 eV) excitation, we ascribe it to hot-carrier transfer to some trap site outside the NC. Photocharging leads to bleaching of steady-state absorption, partial quenching of emission, and additional fast time scales in carrier dynamics due to Auger decay of charged single- and multiexciton states. The degree of photocharging, *f*, saturates at a level that varies from 5 to 15% depending on the sample. The buildup of the population of charged NCs is extremely slow indicating very long, tens of seconds, lifetimes of these charge-separated states. Based on these time scales and the measured onset of saturation of *f* at excitation rates around 0.05−1 photon per NC per ms, we determine that the probability of charging following a photon absorption event is of the order of 10^{-4} to 10^{-3}. The results of these studies have important implications for the understanding of photophysical properties of NCs, especially in the case of time-resolved measurements of carrier multiplication.

KEYWORDS: PbSe nanocrystals · charge separation · charged exciton · trapping · photoluminescence · carrier multiplication · Auger recombination

Size-tunable optical properties of semiconductor nanocrystals (NCs) are central to a variety of prospective applications envisioned for these structures. For example, the size-tunable emission from NCs is part of the basis for their use in light-emitting diodes[1] and as biological labels[2] as well as their potential application as lasing media.[3] Likewise, their size-tunable absorption is attractive for use as, *e.g.*, light harvesters in photovoltaics.[4] It is also through various optical observables that many of the electronic properties of NCs are studied. For example, carrier multiplication (CM), the generation of multiple excitons by absorption of a single photon, has been investigated *via* the transient absorption (TA) and the emission following excitation of NCs with ultraviolet (UV) pulses.[5] However, there are implicit assumptions behind many applications and interpretations of optical studies of NCs, including that the NC interior (core) contains zero net charge and that changing the wavelength of excitation of NCs affects the response of NCs simply through the wavelength and fluence dependence of the generation of neutral excitons.

Over time, a significant amount of experimental evidence has accumulated suggesting that the above assumptions are not always valid. The negative consequences of charging on applications of NCs were recognized in early studies of NCs fabricated by high-temperature precipitation in molten glasses. In particular, the degradation of the optical properties of glass-embedded NCs ("photodarkening") under optical excitation was attributed to accumulation of uncompensated charges formed through Auger recombination (AR) between two electron−hole pairs that resulted in ejection of an electron from the NC and its capture by long-lived centers in the glass.[6,7]

In the case of colloidally synthesized NCs, electrostatic force microscopy (EFM) revealed that NCs immobilized on an insulator−metal substrate can develop a net charge upon photoexcitation, which was explained by tunneling of a photoexcited electron into the metal.[8] More recent EFM studies indicate that the degree of photocharging is dependent on excitation

*Address correspondence to klimov@lanl.gov.

Received for review July 13, 2010 and accepted September 28, 2010.

Published online October 12, 2010. 10.1021/nn1016296

wavelength and occurs more readily for UV photons compared to lower-energy green photons.[9] These observations suggested the existence of additional "hot-electron" ionization pathways that are not accessible from low-energy relaxed electronic states.

Photoinduced charge separation has also been extensively discussed in the context of photoluminescence (PL) intermittency (blinking) observed in studies of individual NCs immobilized on a substrate. Specifically, it was suggested that the transition of the NC to the nonemitting ("dark") state is a result of tunneling of a photoexcited electron to a nearby trap state.[10] As the EFM measurements mentioned above, recent blinking studies suggest that the likelihood of formation of long-lived charge-separated states is higher for higher-frequency photons.[11]

NC photocharging in solution samples has been studied much less extensively. In one example, excitation of water-dispersed CdSe NCs with high-intensity femtosecond pulses resulted in ejection of the electron from the NC, which led to the development of a distinct spectroscopic signature of a solvated electron.[12] This process exhibited a strong dependence on pump power and was explained by two-photon absorption.

The formation of long-lived charge-separated states in well-passivated NCs dissolved in nonpolar organic solvents might be considered unlikely because an ejected charge cannot be easily "stabilized" in a nonpolar medium to prevent its rapid return to the NC core. Contrary to these expectations, our recent CM studies of PbSe NCs prepared in hexane and chloroform indicated clear signatures of photocharging.[13,14] This effect was detected based on pronounced differences in carrier recombination dynamics in stirred versus static samples. Specifically, some of the studied samples excited by UV pulses showed an increased amplitude of the fast decay component due to AR of multiexcitons in the static case compared to the stirred one. This difference was explained by the existence in the NC core of long-lived charges generated as a result of exposure to previous laser pulses. In stirred solutions the effects of photocharging are reduced as charged nanocrystals are swept from the excitation volume between sequential excitation pulses.

In the present report, we give a detailed account of both time-resolved and steady-state measurements of the photocharging of high-quality, well-passivated PbSe NCs in nonpolar solvents. We aim to clarify the trends in the pump-intensity dependence of this process and determine the characteristic lifetimes of charge-separated states and photocharging probabilities. Since a detailed mechanistic understanding of the photocharging or the charge-separation process is still lacking, we emphasize at the outset that terms such as photocharging or photoionization are used to refer simply to a process in which the NC core is left with a net excess charge irrespective of whether the NC as a whole (including ligands) remains neutral. In those samples showing a static-stirred difference, continuous wave (cw) UV excitation of static solutions of NCs yields reduced time-integrated emission intensity (*i.e.*, reduced PL quantum yield) compared to the corresponding emission from stirred solutions. Likewise, compared to stirred solutions, static solutions of NCs show steady-state bleaching when excited with UV light. The fraction of charged NCs estimated from steady-state data is consistent with the estimates from transient PL data. The increase in the fraction of charged NCs with excitation intensity is monotonic but shows saturation at excitation levels well below the typical fluences used in transient measurements of CM. At such low saturation fluences, "dynamical" artifacts due to photocharging may appear to be insensitive to the pump level and thus mimic signatures of true CM. Based on measured onsets for saturation of photocharging (saturation occurs at 0.05−1 photon absorbed per NC per ms) and lifetimes of charge-separated states (tens of seconds), we estimate that the probability of photocharging following a photon absorption event is from 10^{-4} to 10^{-3}. Despite this low probability, very long lifetimes of charge-separated states facilitate the buildup of an appreciable concentration of charged species within a photoexcited sample volume if they are not physically removed between sequential laser pulses, such as by stirring. In these well-passivated samples, photocharging is not observed in the case of lower-energy 1.5 eV excitation, indicating that it is due to direct transfer of an unrelaxed, hot electron or a hole to some trap site outside the NC. These observations of UV-induced photocharging have potentially important implications for numerous applications of NCs as well as interpretation of NC spectroscopic studies and especially quantitative evaluations of CM yields.

RESULTS AND DISCUSSION

Dynamical Signatures of Photocharging. We study oleic acid-capped PbSe NCs with mean radii from ~1.5 to ~3.8 nm and corresponding band gaps (E_g) from 1.085 to 0.617 eV that are much larger than the band gap of bulk PbSe (0.28 eV). Carrier dynamics are studied with ~4 ps resolution by PL upconversion (uPL)[15] and changes in steady-state optical properties by steady-state PL and absorption. Excitation fluences are reported in terms of the average number of photons $\langle N_{abs} \rangle$ absorbed per NC per pump pulse at the peak of the excitation spatial profile or the excitation rate $\langle g_{abs} \rangle$, which is defined as the average number of absorbed photons per NC per unit time.

Time-resolved band-edge PL from a sample with a band gap of 1.085 eV is shown in Figure 1. Panel (a) of this figure displays the dynamics measured under 1.54 eV excitation. For delays much shorter than the single-exciton radiative recombination time (of order of 100 ns to ~1 μs),[16,17] low-fluence excitation at 1.54 eV ($\langle N_{abs} \rangle$

≪ 1) results in nearly "flat" uPL traces on the time scale of our measurements (250 ps) indicating an absence of significant band-edge trapping. At higher fluences ($<N_{abs}> \gtrsim 1$), absorption of multiple photons by single NCs results in the creation of multiple excitons, which decay on characteristic nonradiative AR time scales (biexciton AR time $\tau_{2A} = 29$ ps for this sample).[18] In the case of 1.54 eV excitation, the sample shown in Figure 1a does not show any discernible difference in measured PL dynamics between the static and the stirred solutions.

Figure 1b displays the PL dynamics measured for the same sample under 3.08 eV excitation using very low pump fluence ($<N_{abs}> = 0.045$) for which without CM the vast majority (>97%) of photoexcited NCs would contain single excitons. In this case, however, the stirred sample (open black squares) shows an appreciable fast component, characteristic of AR of multiexcitons. Since this signal develops in the regime of primarily single-photon absorption, it can be attributed to CM.[5,14]

Under 3.08 eV excitation, the trace taken under static conditions (solid red circles in Figure 1b) is distinct from that for the stirred sample. Both traces show a fast initial decay. However, in the static sample, the early time emission is more intense than in the stirred solution, while the signal at long delays is weaker. In the inset of Figure 1b, the differences between the responses of the static and stirred solutions are highlighted by subtracting the constant long-delay uPL signal from the raw experimental traces. In the stirred case, the decay resulting from the subtraction procedure can be fit to a single exponential decay with a 29 ps time constant, which is consistent with AR of biexcitons as inferred from studies using 1.54 eV excitation (Figure 1a). On the other hand, the short-lived PL signal of the static sample is clearly multiexponential, and in addition to the fast initial decay, it shows a slower component. If in a biexponential fit the fast decay time is fixed at 29 ps (biexciton AR time), the slower time constant is ~150 ps.

As has been explained previously, the different dynamics observed under static and stirred solutions excited at 3.08 eV can be understood in terms of photocharging induced by UV light.[13,14] If some fraction of 3.08 eV photon absorption events yields a long-lived (compared to the time between absorption of photons from separate laser pulses) charge-separated state with a nonzero net charge in the core, then subsequent photon absorption creates either a charged single exciton (a trion) or, in the case of CM, a charged biexciton. Compared to NCs with neutral biexcitons, NCs with charged biexcitons should display faster AR ($\tau_{2^*A} < \tau_{2A}$), while trions are expected to undergo AR with a slower time constant than neutral biexcitons ($\tau_{1^*A} > \tau_{2A}$). Simple "statistical" considerations,[19] for example, predict that Auger lifetimes of NC states comprising arbitrary numbers of electrons (N_e) and holes (N_h) in degenerate energy states scale as $1/\tau_A \propto N_e N_h (N_e + N_h - 2)$. In this case, $\tau_{2^*A}/\tau_{2A} = 4/9$, while $\tau_{1^*A}/\tau_{2A} = 4$.

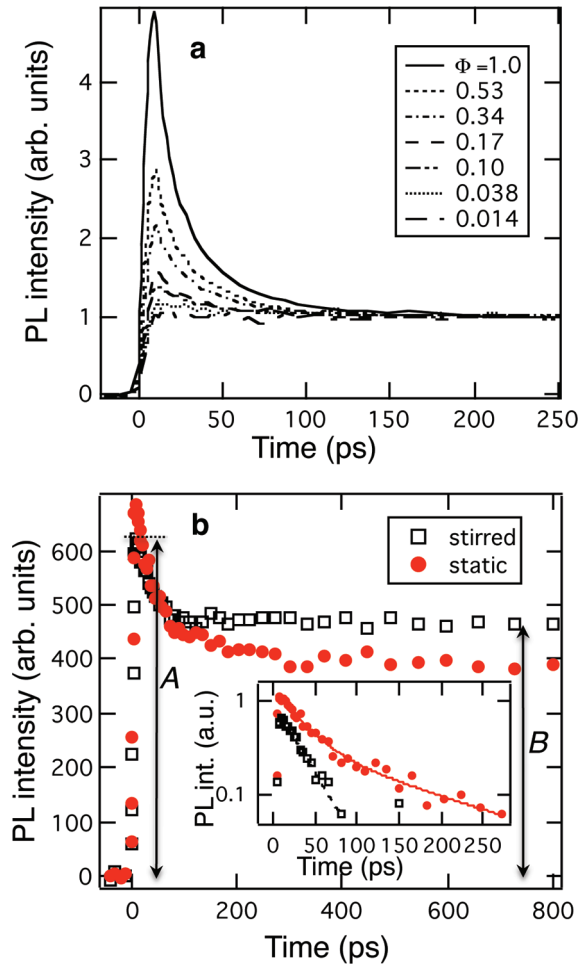

Figure 1. Time-resolved PL measurements of PbSe NCs with $E_g = 1.085$ eV in hexane. (a) Normalized PL traces of stirred solution of NCs under 1.54 eV excitation. The legend indicates the normalized excitation fluences (Φ), where Φ = 1 corresponds to $<N_{abs}> = 1.9$. (b) Raw traces of back-to-back PL measurements under stirred (open black squares) and static (filled red circles) conditions and 3.08 eV excitation at $<N_{abs}> = 0.045$. Inset: PL intensity minus the long-delay value. The dashed and solid curves represent, respectively, single- and biexponential fits to the stirred and static data. The data in the inset is only shown for the first ~300 ps to highlight the differences between the traces, but the fits were performed over the entire 800 ps range of the uPL data.

Differences in the uPL dynamics of stirred and static solutions are expected to develop only if the rate of stirring is such that NCs in a charge-separated state are swept out of the excitation volume before absorbing photons from subsequent laser pulses. The data of Figure 1b appear to be consistent with the above expectations. In particular, the stirred solution under 3.08 eV excitation shows initial fast dynamics that are indistinguishable from the dynamics of neutral biexcitons generated by 1.54 eV excitation. In contrast, for 3.08 eV excitation of the static solution, even low-fluence excitation results in a clearly biexponential uPL decay. The faster decay time is indistinguishable from

the neutral biexciton AR decay time measured under 1.54 eV excitation. However, the slower decay occurs with a time constant *ca*. five times that of the neutral biexciton AR and so is suggestive of trion recombination. As mentioned above, a factor of 4 is expected for the ratio of the trion AR time to the neutral biexciton AR time from the "statistical" arguments of ref 19, while in measurements of electrochemically charged CdSe/CdS core/shell NCs, the reported trion AR times are 7.5(1.7) times that of neutral biexciton AR.[20]

The fact that we see generation of biexcitons by CM in the stirred solution along with signatures of excess core charges in the static sample suggests that in the latter case we should also see a third, still faster decay due to AR of charged biexcitons resulting from CM in charged NCs. The absence of a clear third fast decay time in this sample can be understood as a consequence of our limited temporal resolution, insufficient signal-to-noise ratio, and only a moderate degree of photocharging. However, in static solutions of larger PbSe NCs excited by 3.08 eV photons we did observe decays faster than neutral biexciton AR when stirred solutions only showed AR characteristic of neutral biexcitons.[13,14] These observations along with a quantitative analysis of short- and long-time PL signals suggest that photocharging does not suppress CM, though it does complicate an accurate determination of true CM yields.[14] We point out that this conclusion is at odds with the theoretical results of ref 21, according to which the presence of charges in NCs leads to suppression of CM. The possibility that the larger PbSe NCs showing decays faster than neutral biexciton AR contained multiple excess core charges cannot be ruled out, though, and more detailed studies are required for a quantitative assessment of the effect of excess core charges on CM efficiency.

As with the differences in time scales of PL decay from static and stirred samples, the changes in the amplitudes of short- and long-time PL signals can also be understood based on photocharging arguments. Within the "free-carrier" model,[13,14] the instantaneous PL signal is proportional to the product of the numbers of electrons and holes residing in the NC: $I_{PL} \propto N_e N_h$. This scaling suggests, for example, that charged biexcitons are "brighter" than neutral ones by a factor of 1.5, while trions are twice as "bright" as neutral single excitons. Therefore, short-pulse excitation applied to a charged NC ensemble produces a PL signal that at short times (before AR takes place) is stronger than that from an ensemble of neutral NCs. On the other hand, since carrier decay in charged NCs is dominated by nonradiative AR, photocharged NCs do not contribute to the long-time signal. Therefore, the long-time signal is reduced compared to the signal from neutral NCs. Both of these trends—the increase in the early time PL intensity and the decrease in the late time signal—are observed when we compare PL traces under 3.08 eV excitation for the static and stirred cases (Figure 1b).

To estimate the fraction, f, of NCs in a charge-separated state in a static sample, one can use the difference in long-delay uPL signals for static and stirred cases.[14] At long times following photoexcitation, the NCs with a nonzero net charge decay by AR to a nonemitting single core charge. Therefore, the ratio of the long-delay uPL signal for stirred and static solutions yields the fraction of NCs with neutral cores: $f = 1 - B^*/B$. Applying this expression to the data in Figure 1b, we obtain $f = 0.15$ (the corresponding excitation rate $\langle g_{abs} \rangle$ is 11 ms^{-1}, calculated using $\langle N_{abs} \rangle = 0.045$ and the pulse-to-pulse separation $T = 4$ μs).

We add that the apparent CM efficiency determined from the static solution under 3.08 eV excitation is consistent with photocharging. In the case of PL studies, the quantum efficiency (QE) of photon-to-exciton conversion in neutral NCs can be calculated from the ratio of the early (A) and late (B) signals (Figure 1b) *via* QE = 100%(A/B + 2)/3,[13,14] which can be further used to find the multiexciton yield η = QE − 100%. Since photocharging increases the PL signal at short times after excitation but reduces its magnitude at long times (after AR is completed), the overall effect is an increase in the A/B ratio and an increase in apparent CM QE. For example, based on the stirred measurements in Figure 1b, the CM QE is 109% (η = 9%). On the other hand, the same sample under static conditions shows a higher A/B ratio, which corresponds to an apparent multiexciton yield η^*_{app} = 23% (here and below we denote quantities related to static samples that can be potentially affected by photocharging by an asterisk). A quantitative model proposed in ref 14 allows one to relate the true CM yield to its apparent value in the presence of photocharging using the following expression obtained assuming that true CM yields are identical in neutral and charged NCs ($\eta^* = \eta$): $\eta^*_{app} = [\eta + f(2 + \eta)/3](1 - f)^{-1}$, where f is the fraction of charged NCs in a photoexcited ensemble. For the sample of Figure 1b, η = 9% and $f = 0.15$ yield η^*_{app} = 23%. This value of η^*_{app} is in remarkable agreement with the measurements on the static sample, providing an additional piece of evidence that the difference in dynamics between the static and the stirred solutions is due to photocharging.

We note that we do not observe a correlation between band gap and the fraction of ionized NCs generated by 3.08 eV excitation, as was discussed in detail in ref 14. This implies that photoinduced charge separation is not merely an intrinsic, size-dependent, phenomenon but is affected by other factors, *e.g.*, surface properties of the NCs. Such extrinsic effects are especially pronounced in the case of the two smallest gap (0.617 and 0.630 eV) samples that we studied previously.[13,14] These two samples were of similar size and were prepared by nominally identical synthetic procedures and

dissolved in the same solvent (hexane). Yet, under 3.08 eV excitation the 0.617 eV sample showed little or no static-stirred difference in uPL, while the 0.630 eV sample showed the largest static-stirred difference in uPL of any sample we investigated.

In contrast to the case of 3.08 eV excitation, we do not see signatures of core photocharging in static samples of well-passivated NCs excited with 1.54 eV photons. At the lowest excitation fluences and after initial cooling of hot carriers to the band edges, the uPL signal under 1.54 eV excitation shows "flat" dynamics on the time scale of our measurements. If excess core charges were present, then an initial fast decay due to trion AR would be expected. Also, at higher fluences at which we see the onset of AR, only a single time scale is observed for the initial decay, which is consistent with recombination of neutral biexcitons. Only at very high fluences, when absorption of more than two photons and direct generation of triexcitons and higher order multiexcitons are expected, is a second time scale observed in the uPL traces. For all the samples studied here, though, the ratio of the faster to the slower decay time is within about 25% of the ratio of tri- to biexciton AR times predicted in ref 19 ($\tau_{3A}/\tau_{2A} = 2/9$). We note that the above behaviors are not necessarily observed in poorly passivated samples that exhibited low PL quantum yields and a considerable amplitude of fast initial decay due to surface trapping. Although very few poorly passivated samples were studied, one such sample (static solution) did show the same signatures of photocharging under 1.5 eV excitation that in higher quality samples were only seen at 3.08 eV. Conversely, in a recent study of surface-oxidized NCs, which showed significant trapping under 1.5 eV excitation, no significant static-stirred difference was observed in the corresponding uPL dynamics with 3.08 eV excitation.[22] This indicates that while some of the trap sites accessible from the band-edge NC states may lead to generation of the long-lived charge-separated states others do not.

Steady-State Signatures of Photocharging. We also observe clear signatures of photocharging in steady-state PL and absorption spectra of static solutions, which provides additional means to quantify the fraction of NCs in a charge-separated state. Figure 2a shows the emission spectrum from PbSe NCs with $E_g = 1.085$ eV (same sample as in Figure 1) under 3.08 eV cw excitation. For the static solution the emission is reduced compared to the stirred case, which can be easily understood if we account for the presence of charged NCs. Charged NCs are expected to be nonemissive after AR and only contribute weakly to the total emission because in PbSe NCs the AR lifetimes are orders of magnitude shorter than radiative lifetimes. For a partially charged ensemble of NCs, the ratio of the steady-state PL signal from the static solution (I^*_{PL}) to that from the stirred sample (I_{PL}) thus provides a direct measure of the fraction of neutral NCs, which allows one to determine the

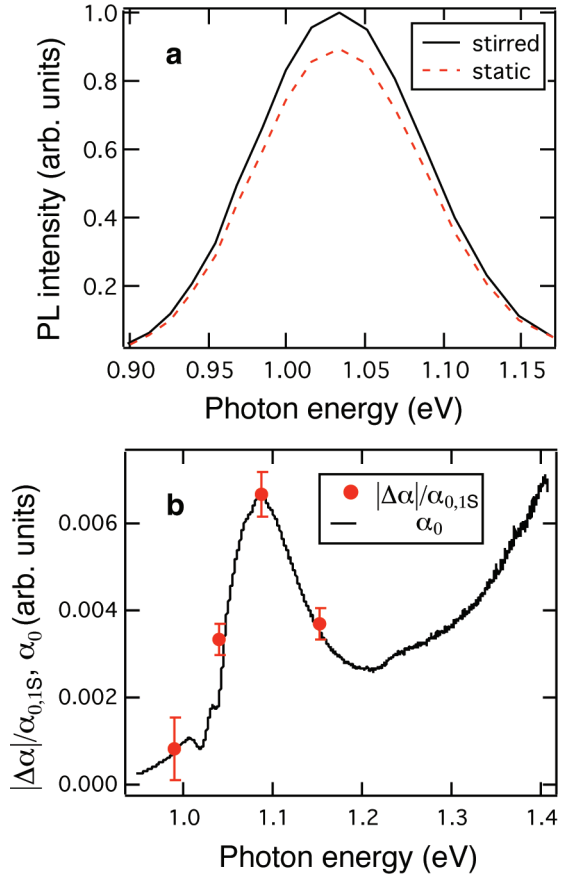

Figure 2. Steady-state absorption and emission spectra for PbSe NCs with $E_g = 1.085$ eV in hexane under 3.1 eV excitation. (a) The cw PL measurements under stirred (solid black curve) and static (dashed red curve) conditions at a photon absorption rate of 0.078 ms^{-1}. Data is normalized to the intensity at the peak of the spectrum from the stirred sample. (b) Absolute value of the change in the steady-state absorption coefficient (filled red circles) of the stirred solution relative to the static solution measured under 3.1 eV excitation by 100 fs pulses at 1 kHz and $<N_{abs}> = 0.5$. The black curve is the absorption coefficient.

degree of photocharging from $f = 1 - I^*_{PL}/I_{PL}$. For the data in Figure 2a, this yields $f = 0.11$ at $<g_{abs}> = 0.078$ ms^{-1}.

The presence of core charges is also evident in steady-state measurements of the band-edge (1S) absorption feature. Specifically, we observe that pulsed excitation of a static solution with 3.08 eV photons results in steady-state bleaching that matches the 1S absorption line shape of a stirred solution (Figure 2b). However, estimating the degree of photocharging in this case is more challenging than in the case of PL measurements. One difficulty is associated with a mismatch of the effective absorption lengths at the excitation and probe wavelengths. The absorption coefficient at the pump wavelength ($\alpha_{0,pump}$) of the PbSe NCs studied here is *ca.* 1 order of magnitude larger than the absorption coefficient at 1.5 eV, which is in turn of the same order as the absorption coefficient at the 1S peak ($\alpha_{0,1S}$). Consequently, absorption measurements were performed under conditions such that 3.08 eV photons

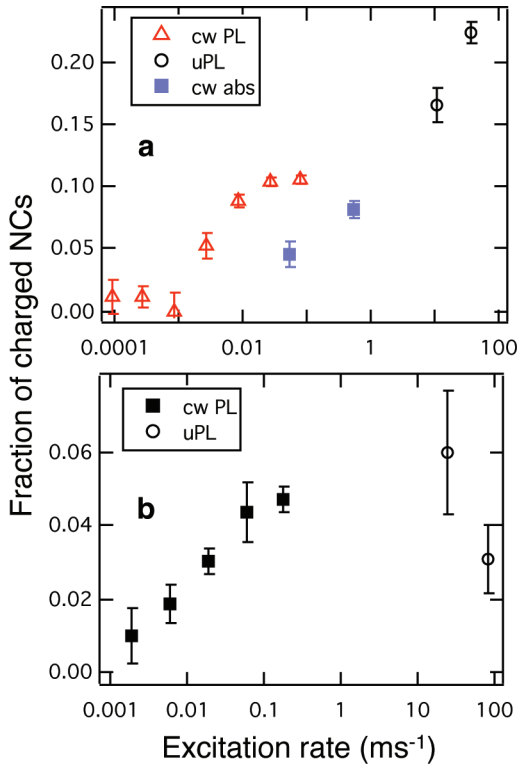

Figure 3. Fraction of photocharged NCs generated by 3.1 eV excitation as a function of excitation rate. (a) Fraction of photocharged NCs (E_g = 1.085 eV, in hexane) as a function of 3.1 eV excitation fluence as determined by cw PL (open red triangles), uPL (open black circles), and cw absorption (filled blue squares). (b) Same as (a), except E_g = 0.925 eV (in hexane) for cw PL (filled black squares) and uPL (open black circles).

penetrated a fraction of the depth of the solution, while the probe photons passed through the samples with little attenuation. If we account for the mismatch of the effective absorption lengths at the pump and probe wavelengths and the 8-fold degeneracy of the 1S states in PbSe NCs,[23,24] then in the case that photocharging depends linearly on UV intensity, we can obtain the following approximate expression that relates the average degree of photocharging in the static sample to the stirred-static difference in the intensity of the transmitted probe light tuned to the 1S resonance ($\Delta I_{T,1S} = I_{T,1S} - I^*_{T,1S}$): $f = 8(|\Delta I_{T,1S}|/I_{T,1S})(\alpha_{0,pump}/\alpha_{0,1S})$. However, this expression only holds for the case of a linear dependence of f on excitation fluence. In the case that photocharging shows saturation at a level f_0, as indicated below, such that a large fraction of the probe path (l is the path length) is saturated and the static-stirred difference is dominated by the saturated region, we then expect $f \approx f_0 = (1/\beta)(8/\alpha_{0,1S}l)\ln(1 + |\Delta I_{T,1S}|/I_{T,1S})$, where β is the fraction of the probe path that is saturated. Applying this expression to the data in Figure 2b for which $\alpha_{0,1S}l = 0.58$ and we estimate $\beta = 2/3$, we obtain $f = 0.08$ ($<g_{abs}> = 0.53$ ms^{-1}).

Figure 3a summarizes the results of our estimates of the fluence dependence of the ionized fraction of NCs determined from transient- and steady-state measurements of the 1.085 eV sample. From steady-state PL, which of all of the techniques allows us to measure static-stirred differences at the lowest fluences, we observe that f goes to 0 as the excitation fluence at ~3.1 eV approaches 0, as expected for photoinduced charging. Further, we observe that the values of f estimated from the different techniques are consistent within a factor of about 2. As illustrated by the example in Figure 3b, this good agreement between different measurements of f across techniques is also seen for other samples.

Since cw PL allows for the most accurate measurements of f down to very low excitation rates, we use this method for the analysis of the pump-intensity dependence of photocharging. In Figure 4a, we present photocharging data for three samples with band gaps of 0.677, 0.925, and 1.085 eV derived from cw PL measurements. These data exhibit several consistent trends. First, we notice that f initially shows a linear growth with $<g_{abs}>$ but then saturates at a level that is different for different samples. This behavior indicates that the charge separation observed here is not mediated by a nonlinear process, such as two-photon absorption (considered, *e.g.*, in ref 12), at least in the range of intensities where the role of multiple photon absorption events is insignificant.

Further, the data in Figure 4a suggest that not all but just a subset of NCs from the ensemble are susceptible to photocharging and that the fraction of these NCs (f_0) defines an upper limit of the degree of charging in a given sample. We also observe that the saturation of f in all samples is achieved at excitation rates of *ca.* 0.05−1 photons per NC per ms. In the case of pulsed PL measurements at a 250 kHz repetition rate, these values translate into very low per-pulse fluences that correspond to an absorption of 0.0004−0.004 photons per pulse per NC. In typical ultrafast CM studies, $<N_{abs}>$ is much greater than the latter values, which would hence correspond to a regime where f is almost pump-intensity independent and close to f_0. This implies that in the limit of the lowest pump intensities typically used to quantify CM yields, the amplitude of dynamical signatures due to charged species (*e.g.*, trions and charged biexcitons) will not decrease but will rather saturate at the value defined by f_0. This mimics the expected behavior for a true CM signal and thus can lead to errors in the experimental determination of QEs.

We have used a simple model for a quantitative analysis of the photocharging results. As discussed above, in this model we assume that only a certain fraction of the NCs in the sample (f_0) can undergo photocharging. We also assume that the rate of formation of charged NCs is proportional to excitation rate ($<g_{abs}>$), while the density of charged species within the excited volume of the sample decays due to recombination of charge-separated electron−hole pairs (characteristic time is τ_{eh}). The above assumptions lead to the

following rate equation for f as a function of time (t), $df(t)/dt = [f_0 - f(t)]\gamma\langle g_{abs}\rangle - f(t)/\tau_{eh}$, which in the steady-state limit reduces to

$$f = f_0\langle g_{abs}\rangle[\langle g_{abs}\rangle + (\gamma\tau_{eh})^{-1}]^{-1} \quad (1)$$

where $\gamma \leq 1$ is the probability of charge separation following a photon absorption event.

We use this expression to analyze photocharging data from Figure 4a (symbols). All three data sets shown can be closely reproduced by the above model (lines in Figure 4a), which allows us to derive both f_0 and $\gamma\tau_{eh}$ (indicated in the plot). The values of f_0 vary from 0.05 for the sample that is least affected by photocharging to 0.14 for the NCs with the largest degree of photocharging, while $\gamma\tau_{eh}$, which determines the onset for saturation ($g_0 = 1/\gamma\tau_{eh}$), is within the range of ~10−250 ms.

To separate contributions from τ_{eh} and γ to the observed saturation thresholds, we measure the lifetime of charge-separated states by analyzing the evolution of the steady-state PL signal after stirring is abruptly stopped. In Figure 4b, we show four PL traces recorded for a sample with $E_g = 0.88$ eV excited at rates from 0.011 to 0.063 ms^{-1}. These traces indicate an extremely slow buildup of the population of charged NCs characterized by a time constant of 39 s. This time provides a direct measure of τ_{eh}. To determine the onset of photocharging saturation for this sample, in Figure 4c, we plot the long-time values of f (laboratory frame time longer than 200 s) as a function of $\langle g_{abs}\rangle$ (red open circles). In the same plot, we also show a high pump-intensity value of f derived from uPL measurements (solid black square). By fitting the experimental data points to eq 1, we obtain $1/g_0 = \gamma\tau_{eh} = 22$ ms. Based on the measured value of τ_{eh}, we further calculate $\gamma = 5.6 \times 10^{-4}$ or 0.056%. For other measured samples, τ_{eh} is in the range of 20−50 s, while γ is from 10^{-4} to 10^{-3}.

Based on the measurements of γ, one can estimate the ionization cross-section (σ_{ion}) of the NCs from the product of the absorption cross-section at the excitation wavelength and γ: $\sigma_{ion} = \gamma\sigma_{abs}$. For the sample in Figure 4b, $\sigma_{ion} = 5 \times 10^{-18}$ cm^{-2} for 3.1 eV excitation. This value suggests that, in a NC exhibiting photocharging and at fluences typically used in time-resolved CM studies ($\langle N_{abs}\rangle < 0.1$), only 1 out of more than 10 000 incident pulses produces a charge-separated state. However, despite a very low probability of photocharging, prolonged exposure to UV radiation can still lead to the buildup of a significant population of charge-separated states because of their extremely long lifetimes.

In our analysis of population decay in the ensemble of charged NCs, we have neglected NC diffusion from the excited volume because the contribution from this process is extremely small. Using the NC diffusion coefficient (D) of ~10^{-6} cm^2 s^{-1} (estimated from the Stokes−Einstein relation for solvent viscosity of ~0.5 mPa s), we obtain that the characteristic NC diffusion time (τ_D) is on the order of hours ($\tau_D \sim d^2/D$) for the excitation spot sizes (d) of ~3 mm used in our measurements. Therefore, the tens of seconds time scale observed for the buildup/decay of the population of charged NCs is not due to NC diffusion but rather to recombination of charge-separated states.

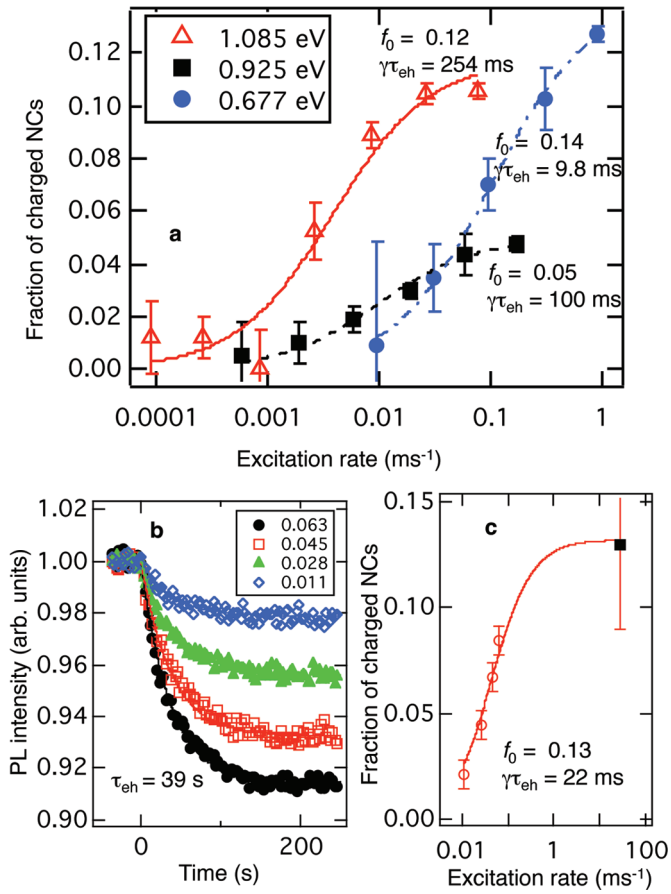

Figure 4. Analysis of onsets for saturation of photocharging and lifetimes of charge-separated states. (a) Fraction of photocharged NCs determined from cw PL as a function of excitation rate (3.08 eV photon energy) for NCs with $E_g = 0.677$ eV in deuterated chloroform (filled blue circles), $E_g = 0.925$ eV in hexane (filled black squares), and $E_g = 1.085$ eV in hexane (open red triangles). Curves are fits to the data using the model described in the text. (b) Slow evolution of the cw PL signal for NCs with $E_g = 0.88$ eV in trichloroethylene in the situation when stirring is abruptly stopped for four different excitation rates indicated in the legend (in ms^{-1}). A gradual reduction of the PL signal is due to the buildup of a population of charged NCs, which occurs with a 39 s time constant. This represents a direct measure of the lifetime of charge-separated states. (c) Steady-state photocharging fractions derived from the data in (b) as a function of excitation rate (open red circles). We also show a high pump-fluence data point obtained from uPL measurements (solid black square). These data indicate $\gamma\tau_{eh} = 22$ ms, which together with results of transient measurements in (b) allows us to determine that the probability of photocharging is $\gamma = 5.6 \times 10^{-4}$ or 0.056%.

Configuration Coordinate Model of Photocharging. The charge separation that is responsible for photocharging induced by UV photons is likely distinct from the common picture of trapping of band-edge excitons by intragap defects as we see a clear photon-energy dependence for such charge separation. In particular, in

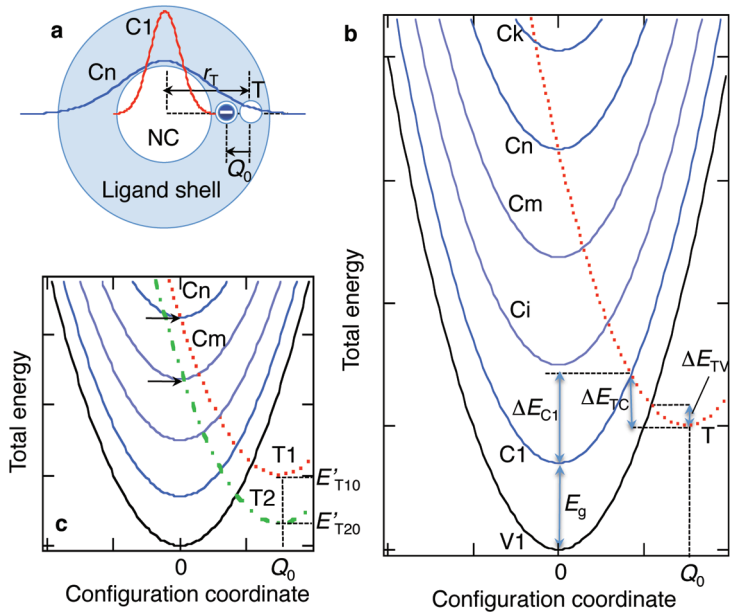

Figure 5. Electron trapping leading to NC charging in a configuration-coordinate representation. (a) A trap center T in the NC ligand shell experiences a displacement Q_0 following electron transfer from the NC conduction-band state. C1 and Cn denote NC wave functions for the low-energy band-edge state (red line) and the excited state (blue line), respectively. While overlap of the NC wave function with the trap state is weak for C1, it increases in the case of Cn. (b) A configuration-coordinate representation of the electronic states in the NC (black and blue solid lines) and the trap state (red dotted line). (c) Same as in (b) but for two trap states (T1 and T2) with two different electronic energies. Arrows mark the barrierless level crossings for T1 and T2.

the case of well-passivated PbSe NCs excited with low-energy (1.5 eV) but above-band gap photons, we see little to no signatures of charge separation, but excitation with 3.1 eV photons does produce in some samples clear signatures of charging. This observation of more efficient photocharging by UV light compared to near-infrared excitation is similar to previous EMF results that indicated wavelength-dependent photocharging of CdSe NCs separated from a conductive substrate by a thin insulating layer.[9] Specifically, the authors of ref 9 suggested that high-energy unrelaxed electrons can tunnel into the conductor *via* a suitable high-energy trap state. Based on our results, a similar process of hot electron transfer to some states outside the NC core is likely possible also in the solution form of NCs. This process is, however, different from the enhanced trapping of excitons created by above-band gap excitation in CdSe NCs studied by Sewall *et al.*, as the latter effect was not associated with formation of a long-lived (tens of seconds) charge-separated state and hence was most likely due to a different type of trapping site that recovers on the time scale of the pulse-to-pulse separation in time-resolved femtosecond measurements.[25]

Given the nonpolar nature of the solvents used in our studies, it is likely that the "hot" charge ejected from the NC core is stabilized at some site in the ligand shell at an appreciable distance from the NC, which complicates its transfer back to the NC and, therefore, results in a long-lived charge-separated state. In Figure 5, we use a configuration-coordinate representation to describe such a photocharging scenario, assuming for the sake of this illustration that the charge escaping the NC is an electron. We consider the situation where the electron acceptor (trapping center) is located somewhere in the ligand shell at a distance r_T from the NC center (Figure 5a). This problem is similar to one analyzed previously by Sercel,[26] who used a configuration-coordinate approach to calculate the rate of electron intraband relaxation due to coupling of a quantum dot excitation to a defect within the surrounding matrix.

In the schematics in Figure 5a, a configuration-coordinate Q is shown as a displacement of the trapping center with respect to the NC. However, one should realize that this is a simplified picture, as in reality Q can describe a much more complex rearrangement of atoms both in surrounding ligand molecules and in a solvent. We assume that following electron transfer from the NC, the trap center experiences a transition to a new equilibrium position Q_0 along the configuration coordinate Q (Figure 5a). This displacement does not affect the electronic energies of quantized NC states (energies E_{Ci} and E_{Vj}, for the conduction and the valence band levels, respectively), but it leads to a change in the electronic energy of the trap level, which for small values of Q can be approximated by a linear dependence: $E_T = E_{T0} - VQ$. Here, E_{T0} is the trapped electron energy for $Q = 0$, and V is the matrix element that couples center displacement to electron motion. In this model, the total energy of the system (the sum of the electronic energy and the energy of center vibrations) for the trapped electron and the electron in the quantized NC state can be presented, respectively, as $E_{tot,T} = E'_{T0} + (\hbar\omega/2)(Q - Q_0)^2$ and $E_{tot,Cn} = E_{Cn} + (\hbar\omega/2)Q^2$, where ω is the frequency of acceptor vibrations along the configuration coordinate, $E'_{T0} = E_{T0} - V^2/(2\hbar\omega)$, and $Q_0 = V/(\hbar\omega)$ is the "displaced" coordinate.

In Figure 5b, we use the above expressions to show the energies of the NC valence band-edge state (V1), a few NC conduction band states (C1, C2, ..., C*i*), and the trap state (T). In this plot, the trap state is positioned in such a way that it is separated from the lowest-energy conduction band state (C1) by a sizable potential barrier (ΔE_{C1}), which makes it difficult for the relaxed C1 electron to access it. On the other hand, the height of the potential barrier gets progressively smaller with increasing energy of the NC electron level. For an excited state of a sufficiently high energy, the trapping process can

become "barrierless," as illustrated in Figure 5b using state Cn as an example. As the electron energy is increased further (see, *e.g.*, state Ck in Figure 5b), the energy barrier for carrier trapping starts to increase again, which corresponds to charge transfer in the inverted regime.[27] This reappearing barrier inhibits direct carrier trapping from a photoexcited high-energy state. However, even in this case, electron trapping can still be barrierless if the electron first relaxes to the Cn state (due, *e.g.*, to coupling to NC lattice vibrations[28] or electron−hole energy transfer)[29] and then is transferred to the trap site.

In addition to a reduced barrier, direct trapping from a higher-energy NC level is facilitated by increasing leakage of quantized states into the region outside the NC, which increases their overlap with the wave function of the trap state (see schematic illustration in Figure 5a). Specifically, using approaches previously developed for the problem of charge trapping at localized defect states in bulk semiconductors (see, *e.g.*, ref 30), one can show that the trapping rate from the state C*i* ($W_{Ci,T}$) in the high-temperature limit can be expressed as $W_{Ci,T} = (\omega/2\pi)\, P_{Ci,T} \exp(-\Delta E_{Ci}/k_BT)$. Here, $P_{Ci,T}$ is a factor that, in the weak-coupling, nonadiabatic regime (most likely realized here given the very low probabilities of photocharging) is proportional to the square of the modulus of the matrix element of the C*i*−T interaction and hence directly depends on the overlap between the wave functions of the NC and the trap states. We point out that the probability of trapping does not vanish even in the limit of low temperatures ($k_BT \ll \hbar\omega$), as in this case, the transition to the trap site can occur *via* quantum-mechanical tunneling (see, *e.g.*, ref 26).

The above model offers a possible rationalization of our photocharging results. One experimental observation is that the well-passivated samples studied here do not display photocharging at 1.5 eV excitation but exhibit signatures of photocharging if excited at 3.1 eV. This result implies the existence of an energy threshold for photocharging. Based on our model, we can suggest that this threshold develops as a result of competition between intraband relaxation (rate W_{rel}) and trapping. Specifically, when the NCs are excited into a low-energy state, $W_{Ci,T}$ is smaller than W_{rel}, and therefore, most of the photoexcited electrons rapidly relax into the ground C1 state, which only weakly interacts with the trap state and is further separated from it by a large potential barrier (ΔE_{C1}); both of these factors inhibit trapping. On the other hand, the trapping probability increases with increasing excitation energy, which is a result of two factors: the reduction of the trapping barrier (this leads to the increase of the exponential factor in $W_{Ci,T}$) and the increase of the wave function overlap between the NC and the trap states (this increases $P_{Ci,T}$). Therefore, when the energy of the photoexcited electron increases, one eventually can have a situation where $W_{Ci,T}$ becomes an appreciable fraction of W_{rel} so that the signal resulting from charged NCs becomes resolvable experimentally; this will be observed as a spectroscopic threshold for photocharging.

The configuration-coordinate model in Figure 5b also allows one to understand the very long lifetimes of charge-separated states. After relaxation into a vibrational minimum of the trap state, the electron is separated from the valence-band state by a large potential barrier, ΔE_{TV}, which greatly reduces the exponential factor in the transfer rate, and hence, the likelihood of trapped electron recombination with a valence-band hole. The return of the electron to the conduction band is also inhibited by an even bigger potential barrier ΔE_{TC}. Further, neither of the band-edge NC states (C1 and V1) significantly leaks outside the NC, and therefore, they only weakly couple to the T-state. This leads to an additional reduction of the "detrapping" probability and hence very long, tens of seconds, lifetimes of the trapped electrons.

The above considerations also explain sample-to-sample variability in the degree of photocharging as well as nonuniformity in photocharging across the NC ensemble (*e.g.*, the existence of "chargeable" and "nonchargeable" NCs). Given the complexity of the NC ligand shell, one might expect the existence of a variety of trapping sites occurring at different separations from the NC and characterized by different electronic energies, vibrational frequencies, and coupling matrix elements. These differences are expected to lead to variations in parameters, such as r_T, E'_{T0}, V, and Q_0 and, hence, the height of the potential barriers that control trapping/detrapping as well as the coupling strength of states in the NCs to trap states.

To illustrate this variability, in Figure 5c we show two trap states (T1 and T2) that are characterized by two different energy minima $E'_{T20} < E'_{T10}$. We further assume that the photocharging threshold is located near the energy where NC and trap levels exhibit a barrierless crossing (marked by arrows in Figure 5c).[31] Because of a smaller value of E'_{T0}, the T2 trap exhibits a lower trapping threshold (corresponding to the Cm state) than the T1 trap (corresponding to the Cn state). If the NCs are photoexcited into the Cm state, the subset of particles with the T2 trap state will exhibit photocharging, while the particles having the T1 trap will not. As a result, some of the NCs in the ensemble will behave as "chargeable" and others as "unchargeable." An interesting conjecture from this model is also that the "unchargeable" NCs will become "chargeable" if one increases the photon energy to excite the electron into the Cn state. Thus, one might expect that the degree of photocharging will exhibit a continuous growth with photon energy above the threshold energy due to increasing availability of potential trap sites.

CONCLUSIONS

In this report, we have presented a detailed comparison of the signatures of UV-induced photocharging of solutions of colloidal semiconductor nanocrystals (NCs) across a range of transient- and steady-state techniques. UV excitation leads to partial quenching of photoluminescence (PL) and steady-state bleaching of the interband 1S absorption peak. The fraction of charged NCs, *f*, in a photoexcited ensemble is consistent across the techniques. In contrast, in these well-passivated samples, photocharging is not discernible under excitation with 1.5 eV photons, indicating that this process is mediated by direct transfer of a hot carrier (an electron or a hole) to some trap site outside the NC.

The degree of photocharging initially grows linearly with pump fluence but then rapidly saturates at a certain value (from 5 to 15% in our measurements) defined by the fraction of "chargeable" NCs in the ensemble. This saturation occurs at excitation rates as low as ~0.1 photon per NC per ms or ~0.0004 photon per NC per pulse in uPL measurements. The observed saturation thresholds and the measured lifetimes of charge-separated states (tens of seconds) imply that the probability of photocharging following a photon absorption event is from 10^{-4} to 10^{-3}. Our observations can be understood in terms of a configuration-coordinate approach, which allows us to rationalize the spectral dependence of photocharging, the long lifetimes of charged states, and the existence of "chargeable" and "unchargeable" NCs as well as the sample-to-sample variability in the degree of photocharging.

Our results have important implications for spectroscopic studies of NCs and especially studies of the carrier multiplication (CM) process. Despite a low probability of photocharging ($<10^{-3}$) observed for samples under investigation (well-passivated NCs in nonpolar solvent), the extremely long lifetime of the charge-separated state facilitates accumulation of charged NCs within the excitation volume if the sample is not refreshed (*via*, *e.g.*, stirring) between sequential laser pulses. Further, in CM measurements, excitation fluences are normally greater than the onset for saturation of *f*. Therefore, the dynamical signatures due to photocharging are expected to be almost independent of excitation intensity, which thus mimics the behavior due to true CM. If not accounted for, the effects of photocharging can lead to errors in quantitative measurements of CM efficiencies. This may represent an especially serious problem in the case of NC films in which simple means for mitigating photocharging, such as sample stirring, are not readily available. In addition to complicating the analysis of CM results, the effects of uncontrolled photocharging are deleterious to many applications of NCs, as Auger recombination of carriers with pre-existing charges opens additional channels for fast nonradiative population losses.

METHODS

Oleic acid-capped PbSe NCs were prepared as described previously.[32,33] The NCs were dissolved in either hexane, deuterated chloroform, or trichloroethylene (TCE) and diluted to an optical density of 0.1−0.3 at 1.55 eV in a 1 mm thick cuvette with an airtight seal in an argon atmosphere. Based on prescreening using time-resolved PL measurements, we only select well-passivated samples that do not exhibit any discernible fast-decay component due to surface trapping of band-edge excitons.

Time-resolved PL measurements were performed as previously described.[14] Samples were excited using the 1.54 eV fundamental or the 3.08 eV second-harmonic outputs from a Ti:sapphire amplifier operating at 250 kHz. Emission due to recombination of band-edge carriers was temporally resolved using PL upconversion (uPL).[15] In this method, PL arising from short-pulse excitation (derived from 0.2−3 ps stretched pulses at the fundamental laser frequency) of NC solutions was spatially and temporally overlapped with a gate pulse of 1.54 eV photons (derived from the same fundamental radiation) in a nonlinear β-barium borate (BBO) crystal. Visible photons produced by sum-frequency generation between the PL and gate pulses were sent through a monochromator and detected with a photomultiplier tube followed by photon-counting electronics. The width of the monochromator slit was set to correspond to a resolution of ~50 meV in the spectral range of NC emission, which is comparable to the width of the band-edge emission peak and much larger than spectral shifts due to exciton−exciton interactions.[34,35]

Steady-state measurements of PL were performed by exciting samples with a cw diode laser at 1.53 or 3.08 eV. The excitation spot diameter was about 0.6 mm at 1.53 eV and 3 mm at 3.08 eV. The PL was detected with a liquid nitrogen-cooled InSb detector after spectral filtering through Si or glass filters and a monochromator. Detection was performed by lock-in amplification while mechanically chopping the laser beam at 3 kHz.

Long-lived photoinduced changes in steady-state absorption were studied using probe radiation from a Xe lamp spectrally filtered so that only near-infrared light was incident onto the sample. The transmitted probe was passed through a monochromator and detected with a Ge photodiode. The probe light was chopped at 250 Hz and measured *via* lock-in detection, while the sample was excited at 3.1 eV by the frequency-doubled output of a 100 fs laser operating at 1 kHz.

Spectrally filtered radiation from Xe and W lamps was also used in studies of lifetimes of charge-separated states. These lifetimes were measured by monitoring a slow evolution (laboratory time frame) of the PL signal after sample stirring was abruptly stopped. This allowed for the population of charged NCs in the excited volume to gradually build up, which led to the reduction of the PL signal. The size of the excitation spot in these measurements was ~3 mm.

Excitation fluences in time-resolved measurements are reported in terms of the average number of photons, $\langle N_{abs} \rangle$, absorbed per NC per pump pulse at the peak of the pulse spatial profile at the entrance face of the sample: $\langle N_{abs} \rangle = j_p \sigma_{abs}$, where j_p is the measured per-pulse pump fluence in units of photons per unit area, and σ_{abs} is the absorption cross-section. The absorption cross-sections of PbSe NCs at 3.08 eV were derived from the reported values of Moreels *et al.*[36] by introducing a correction for the difference in the refractive indexes of the solvents. For steady-state measurements or when comparing transient- and steady-state experiments, we express the pump intensity in terms of excitation rate, $\langle g_{abs} \rangle$, which is defined as the average number of absorbed photons per NC per unit time. In the case of pulsed excitation, $\langle g_{abs} \rangle$ is related to $\langle N_{abs} \rangle$ by

$\langle g_{abs} \rangle = \langle N_{abs} \rangle T^{-1} = j_p \sigma_{abs} T^{-1}$, where T is the pulse-to-pulse temporal separation.

Acknowledgment. V.I.K, M.S., and J.M.P. acknowledge support of the Center for Advanced Solar Photophysics, an Energy Frontier Research Center funded by the United States Department of Energy (U.S. DOE), Office of Science, Office of Basic Energy Sciences (BES). J.A.M. and J.J. were supported by the Chemical Sciences, Biosciences and Geosciences Division of BES, U.S. DOE. L.A.P. is supported by Los Alamos LDRD program.

REFERENCES AND NOTES

1. Colvin, V. L.; Schlamp, M. C.; Alivisatos, A. P. Light-Emitting-Diodes Made from Cadmium Selenide Nanocrystals and a Semiconducting Polymer. *Nature* **1994**, *370*, 354–357.
2. Bruchez, M.; Moronne, M.; Gin, P.; Weiss, S.; Alivisatos, A. P. Semiconductor Nanocrystals as Fluorescent Biological Labels. *Science* **1998**, *281*, 2013–2016.
3. Klimov, V. I.; Mikhailovsky, A. A.; Xu, S.; Malko, A.; Hollingsworth, J. A.; Leatherdale, C. A.; Eisler, H. J.; Bawendi, M. G. Optical Gain and Stimulated Emission in Nanocrystal Quantum Dots. *Science* **2000**, *290*, 314–317.
4. Kamat, P. V. Meeting the Clean Energy Demand: Nanostructure Architectures for Solar Energy Conversion. *J. Phys. Chem. C* **2007**, *111*, 2834–2860.
5. Schaller, R. D.; Klimov, V. I. High Efficiency Carrier Multiplication in PbSe Nanocrystals: Implications for Solar Energy Conversion. *Phys. Rev. Lett.* **2004**, *92*, 186601.
6. Ekimov, A. I.; Efros, A. L. Nonlinear Optics of Semiconductor-Doped Glasses. *Phys. Status Solidi B* **1988**, *150*, 627–633.
7. Chepic, D. I.; Efros, A. L.; Ekimov, A. I.; Ivanov, M. G.; Kharchenko, V. A.; Kudriavtsev, I. A.; Yazeva, T. V. Auger Ionization of Semiconductor Quantum Drops in a Glass Matrix. *J. Lumin.* **1990**, *47*, 113–127.
8. Krauss, T. D.; Brus, L. E. Charge, Polarizability, and Photoionization of Single Semiconductor Nanocrystals. *Phys. Rev. Lett.* **1999**, *83*, 4840–4843.
9. Li, S.; Steigerwald, M. L.; Brus, L. E. Surface States in the Photoionization of High-Quality CdSe Core/Shell Nanocrystals. *ACS Nano* **2009**, *3*, 1267–1273.
10. Nirmal, M.; Dabbousi, B. O.; Bawendi, M. G.; Macklin, J. J.; Trautman, J. K.; Harris, T. D.; Brus, L. E. Fluorescence Intermittency in Single Cadmium Selenide Nanocrystals. *Nature* **1996**, *383*, 802–804.
11. Knappenberger, K. L.; Wong, D. B.; Romanyuk, Y. E.; Leone, S. R. Excitation Wavelength Dependence of Fluorescence Intermittency in CdSe/ZnS Core/Shell Quantum Dots. *Nano Lett.* **2007**, *7*, 3869–3874.
12. Son, D. H.; Wittenberg, J. S.; Alivisatos, A. P. Multielectron Ionization of CdSe Quantum Dots in Intense Femtosecond Ultraviolet Light. *Phys. Rev. Lett.* **2004**, 92.
13. McGuire, J. A.; Joo, J.; Pietryga, J. M.; Schaller, R. D.; Klimov, V. I. New Aspects of Carrier Multiplication in Semiconductor Nanocrystals. *Acc. Chem. Res.* **2008**, *41*, 1810–1819.
14. McGuire, J. A.; Sykora, M.; Joo, J.; Pietryga, J. M.; Klimov, V. I. Apparent Versus True Carrier Multiplication Yields in Semiconductor Nanocrystals. *Nano Lett.* **2010**, *10*, 2049–2057.
15. Shah, J. Ultrafast Luminescence Spectroscopy Using Sum Frequency Generation. *IEEE J. Quantum Electron.* **1988**, *24*, 276–288.
16. Du, H.; Chen, C. L.; Krishnan, R.; Krauss, T. D.; Harbold, J. M.; Wise, F. W.; Thomas, M. G.; Silcox, J. Optical Properties of Colloidal PbSe Nanocrystals. *Nano Lett.* **2002**, *2*, 1321–1324.
17. Wehrenberg, B. L.; Wang, C.; Guyot-Sionnest, P. Interband and Intraband Optical Studies of PbSe Colloidal Quantum Dots. *J. Phys. Chem. B* **2002**, *106*, 10634–10640.
18. Klimov, V. I.; Mikhailovsky, A. A.; McBranch, D. W.; Leatherdale, C. A.; Bawendi, M. G. Quantization of Multiparticle Auger Rates in Semiconductor Quantum Dots. *Science* **2000**, *287*, 1011–1013.
19. Klimov, V. I.; McGuire, J. A.; Schaller, R. D.; Rupasov, V. I. Scaling of Multiexciton Lifetimes in Semiconductor Nanocrystals. *Phys. Rev. B: Condens. Matter Mater. Phys.* **2008**, *77*, 195324.
20. Jha, P. P.; Guyot-Sionnest, P. Trion Decay in Colloidal Quantum Dots. *ACS Nano* **2009**, *3*, 1011–1015.
21. Isborn, C. M.; Prezhdo, O. V. Charging Quenches Multiple Exciton Generation in Semiconductor Nanocrystals: First-Principles Calculations on Small PbSe Clusters. *J. Phys. Chem. C* **2009**, *113*, 12617−12621.
22. Sykora, M.; Koposov, A. Y.; McGuire, J. A.; Schulze, R. K.; Tretiak, O.; Pietryga, J. M.; Klimov, V. I. Effect of Air Exposure on Surface Properties, Electronic Structure, and Carrier Relaxation in PbSe Nanocrystals. *ACS Nano* **2010**, *4*, 2021–2034.
23. Kang, I.; Wise, F. W. Electronic Structure and Optical Properties of PbS and PbSe Quantum Dots. *J. Opt. Soc. Am. B* **1997**, *14*, 1632–1646.
24. Schaller, R. D.; Petruska, M. A.; Klimov, V. I. Tunable near-Infrared Optical Gain and Amplified Spontaneous Emission Using PbSe Nanocrystals. *J. Phys. Chem. B* **2003**, *107*, 13765–13768.
25. Sewall, S. L.; Cooney, R. R.; Anderson, K. E. H.; Dias, E. A.; Sagar, D. M.; Kambhampati, P. State-Resolved Studies of Biexcitons and Surface Trapping Dynamics in Semiconductor Quantum Dots. *J. Chem. Phys.* **2008**, 129.
26. Sercel, P. C. Multiphonon-Assisted Tunneling through Deep Levels - a Rapid Energy-Relaxation Mechanism in Nonideal Quantum-Dot Heterostructures. *Phys. Rev. B: Condens. Matter Mater. Phys.* **1995**, *51*, 14532–14541.
27. Marcus, R. A.; Sutin, N. Electron Transfers in Chemistry and Biology. *Biochim. Biophys. Acta* **1985**, *811*, 265–322.
28. Schaller, R. D.; Pietryga, J. M.; Goupalov, S. V.; Petruska, M. A.; Ivanov, S. A.; Klimov, V. I. Breaking the Phonon Bottleneck in Semiconductor Nanocrystals Via Multiphonon Emission Induced by Intrinsic Nonadiabatic Interactions. *Phys. Rev. Lett.* **2005**, *95*, 196401.
29. Klimov, V. I.; McBranch, D. W. Femtosecond 1p-to-1s Electron Relaxation in Strongly Confined Semiconductor Nanocrystals. *Phys. Rev. Lett.* **1998**, *80*, 4028–4031.
30. Ridley, B. K. *Quantum Processes in Semiconductors*, 1st ed.; Oxford University Press: Oxford, U.K., 1982; p 286.
31. This assumption is a simplification to help one to picture the position of the threshold when dealing with the configuration-coordinate approach. As discussed in the main text, the actual position of the photocharging threshold should be determined based on an analysis of the intraband relaxation and trapping rates.
32. Pietryga, J. M.; Werder, D. J.; Williams, D. J.; Casson, J. L.; Schaller, R. D.; Klimov, V. I.; Hollingsworth, J. A. Utilizing the Lability of Lead Selenide to Produce Heterostructured Nanocrystals with Bright, Stable Infrared Emission. *J. Am. Chem. Soc.* **2008**, *130*, 4879–4885.
33. Joo, J.; Pietryga, J. M.; McGuire, J. A.; Jeon, S.-H.; Williams, D. J.; Wang, H.-L.; Klimov, V. I. A Reduction Pathway in the Synthesis of PbSe Nanocrystal Quantum Dots. *J. Am. Chem. Soc.* **2009**, *131*, 10620–10628.
34. Klimov, V. I. Spectral and Dynamical Properties of Multilexcitons in Semiconductor Nanocrystals. *Annu. Rev. Phys. Chem.* **2007**, *58*, 635–673.
35. Trinh, M. T.; Houtepen, A. J.; Schins, J. M.; Hanrath, T.; Piris, J.; Knulst, W.; Goossens, A.; Siebbeles, L. D. A. In Spite of Recent Doubts Carrier Multiplication Does Occur in PbSe Nanocrystals. *Nano Lett.* **2008**, *8*, 1713–1718.
36. Moreels, I.; Lambert, K.; De Muynck, D.; Vanhaecke, F.; Poelman, D.; Martins, J. C.; Allan, G.; Hens, Z. Composition and Size-Dependent Extinction Coefficient of Colloidal PbSe Quantum Dots. *Chem. Mater.* **2007**, *19*, 6101–6106.